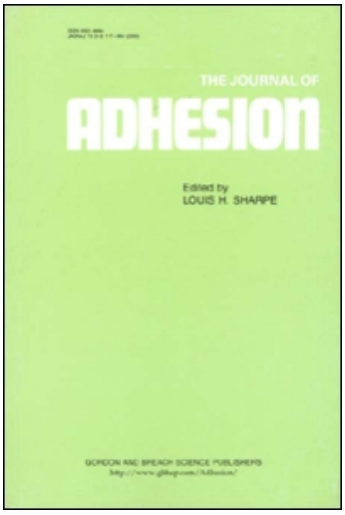


**The Journal of Adhesion**
Publication details, including instructions for authors and subscription information:
http://www.informaworld.com/smpp/title~content=t713453635

# Experiments on contact of a loop with a substrate to measure work of adhesion

Jia Qi[a]; David A. Dillard[a]; Raymond H. Plaut[b]; John G. Dillard[c]
[a] Center for Adhesive and Sealant Science, Engineering Science and Mechanics Department, Virginia Polytechnic Institute and State University, Blacksburg, Virginia, USA [b] Center for Adhesive and Sealant Science, Civil and Environmental Engineering Department, Virginia Polytechnic Institute and State University, Blacksburg, Virginia, USA [c] Center for Adhesive and Sealant Science, Chemistry Department, Virginia Polytechnic Institute and State University, Blacksburg, Virginia, USA

Online publication date: 08 September 2010

**To cite this Article** Qi, Jia , Dillard, David A. , Plaut, Raymond H. and Dillard, John G.(2003) 'Experiments on contact of a loop with a substrate to measure work of adhesion', The Journal of Adhesion, 79: 6, 559 — 579
**To link to this Article: DOI:** 10.1080/00218460309543
**URL:** http://dx.doi.org/10.1080/00218460309543

*The Journal of Adhesion*, 79: 559–579, 2003

ISSN: 0021-8464
DOI: 10.1080/00218460390201329

Taylor & Francis
Taylor & Francis Group

# EXPERIMENTS ON CONTACT OF A LOOP WITH A SUBSTRATE TO MEASURE WORK OF ADHESION

**Jia Qi**
**David A. Dillard**
Center for Adhesive and Sealant Science, Engineering Science and Mechanics Department, Virginia Polytechnic Institute and State University, Blacksburg, Virginia, USA

**Raymond H. Plaut**
Center for Adhesive and Sealant Science, Civil and Environmental Engineering Department, Virginia Polytechnic Institute and State University, Blacksburg, Virginia, USA

**John G. Dillard**
Center for Adhesive and Sealant Science, Chemistry Department, Virginia Polytechnic Institute and State University, Blacksburg, Virginia, USA



*A technique for characterizing surface energies of solid materials is investigated experimentally and numerically. A narrow strip is bent into a loop, pushed into contact with a flat substrate, and then pulled off the substrate. Provided the loop is sufficiently flexible, the size of the contact zone during this process was expected to depend on the interfacial interactions. Larger adhesion forces should tend to increase the contact size, in a manner analogous to the JKR technique. The experiments involve a poly (dimethyl siloxane) (PDMS) loop and glass substrates with various coatings. Anticlastic bending of the loop affects the contact zone. Hysteresis is observed between the loading and unloading data. A three-dimensional finite element analysis is conducted in which adhesion forces are not included, and results from a two-dimensional elastica model of the loop are*

Received 25 September 2001; in final form 22 October 2002.

This research was supported by the National Science Foundation under Grant No. CMS-9713949. The authors would like to acknowledge helpful input from Manoj Chaudhury (Lehigh University), Matt Tirrell's group (then of the University of Minnesota), Ken Shull (Northwestern University), Ken Liechti and Greg Swadener (University of Texas at Austin), and Al Pocius (3M). Finally, the reviewers provided very valuable feedback, and their careful reviews and responses are greatly appreciated.

Current address of Jia Qi is Cooper Tire and Rubber Company, Findlay, Ohio, USA.

Address correspondence to David A. Dillard, Engineering Science and Mechanics Department, 0219, Virginia Polytechnic Institute and State University, Blacksburg, VA 24061, USA. E-mail: dillard@vt.edu

*utilized for comparison purposes. The contact zone appears to be insensitive to the adhesive interactions between the loop and the substrate for the systems studied.*

**Keywords:** Work of adhesion; Loop; Contact experiments; Finite element analysis; Elastica; JKR technique; Surface energy of solids



## INTRODUCTION

The measurement of the work of adhesion is of significant technical interest for a variety of applications, ranging from a basic understanding of material behavior to the practical aspects associated with making strong, durable adhesive bonds. Because the surface energies of liquids are sufficient to control or alter their shapes, the surface energies of liquids can be readily determined through several methods [1]. Quantifying surface energies of solid surfaces has proven to be more problematic, however, because the surface energies of solids are usually not sufficient to overcome the inherent stiffness and significantly alter the shape. In 1971, Johnson, Kendall, and Roberts [2] published their seminal study in which they successfully used elastomeric spheres to measure the surface energies of solid surfaces. This JKR technique has now been widely adopted to measure surface interactions between a variety of solid surfaces. With few exceptions, however, the method has continued to utilize an elastomer as one of the surfaces being investigated. Elastomers are sufficiently soft that spherical or cylindrical caps brought into contact with another solid can deform appreciably due to the work of adhesion forces that act across the interface. If one wants to measure the work of adhesion between two solids, neither of which is elastomeric, one may coat an elastomeric cap with a thin layer of one of the materials of interest [3], or utilize high-precision techniques to characterize the small deformations that result [4]. Membrane configurations have also been suggested [5], although experimental implementation has not been reported.

The objective of this study is to investigate a novel technique using a thin, flexible loop to measure the work of adhesion between solid materials. The concept involves the use of a "soft" structure when the material or materials involved are not "soft" and not amenable to JKR testing. Experimental results are reported, as well as results from a finite element analysis.

Plaut *et al.* [6, 7] previously analyzed a promising system comprised of a thin, flexible strip that is bent to form a loop with its ends clamped

a fixed distance apart. Their analysis assumed that the strip is an elastica, *i.e.*, a flexible, inextensible beam whose bending moment is proportional to the curvature. The equations of equilibrium were solved numerically using a shooting method for the case of a loop approaching and being compressed on a rigid substrate. The effect of adhesion attractions was not included in and one study [6]. In the subsequent study [7], two types of analyses were conducted to examine how the work of adhesion affects the contact length between the loop and the flat substrate, as well as the forces and the shape of the loop. The first was a JKR-type of analysis, in which there was no cohesive zone outside the region of contact, and the adhesive forces were represented by a moment at the edges of the contact region. The value of this moment was chosen such that the total energy (including the adhesion energy) was minimized, leading to stable equilibrium states. The second was a Derjaguin, Muller, and Toporov (DMT)-type of analysis [8], in which there was a cohesive zone from the edge of the contact region until the gap between the loop and the substrate reached a specified value, and a constant (Dugdale-Maugis) attractive force was assumed to act in that zone [9].



## EXPERIMENTS

Experimental implementation involves bending a strip of the desired probe material into a loop and clamping the ends at a fixed separation distance. The loop is then pushed onto a flat substrate of the desired material, recording the force, displacement, and contact length. Finally, the loop is gradually withdrawn from the substrate, again recording the same parameters. If the loop is sufficiently flexible, we had anticipated that interfacial attraction forces should be sufficient to noticeably deform the loop, as had in fact been predicted analytically [7].

Original plans for the loop method had been to use thin flexible polymeric strips that were not necessarily elastomeric. This could potentially avoid the typical implementation of the JKR probe in which at least one of the materials is elastomeric. Trials of polyethylene loops, however, revealed that intimate contact was not being made between the loop and a smooth glass surface. Subsequent tests were thus performed using loops cut from films of poly (dimethyl siloxane) (PDMS), a common, elastomeric material for JKR-type measurements. The loops were made of SYLGARD® 184 silicone elastomer (PDMS) provided by the Dow Corning Company (Midland, Michigan, USA). This product contains a silicone base and curing agents, and is supplied in a two-part kit comprised of liquid components. The base and the curing agent were mixed in a ratio of 10 parts base to one part curing agent by

weight with gentle stirring for about 10 min to minimize the amount of entrapped air. The mixture rested in air for 30 min to remove the air bubbles before use, and was then poured on a glass plate that had been cleaned with acetone. A doctor blade was used to spread the liquid to a uniform thickness. In the curing process, the temperature was raised from room temperature to 100°C at a rate of 5°C/min, maintained for 1 h, and then decreased to room temperature at the same rate. The product was a homogeneous, transparent, flexible film with thickness of about 0.2 mm. Loop specimens were cut from the cured PDMS films, with nominal dimensions of 15 mm × 1 mm.

Various substrates were selected: glass plates coated with PDMS, acetone-washed glass plates, polycarbonate (PC) plates, and a commercial cellulose acetate substrate. After preparation, all the substrates, as well as the elastomer films, were stored in a desiccator at room temperature with relative humidity (RH) controlled at 30%. In addition, a series of coated glass plates was also studied to determine the influence of surface chemistry on the contact process. The glass surfaces were cleaned with acetone or coated with gold or copper, or modified using a silane coupling agent. The glass was cleaned by wiping the surface with a tissue that had been saturated with acetone. The glass specimen was allowed to dry in air at room temperature. For the gold- or copper-coated glass, metal films of at least 200 Å were deposited by sputtering the metal onto acetone-cleaned glass. The sputtering was carried out using an Edwards model S150B sputter coater (Edwards High Vacuum, Crawleg, W. Sussex, UK). Sputtering was accomplished in an argon atmosphere, and the Ar pressure was approximately 5 millibar. The DC potential for sputtering was 2 kV.



To investigate a silane-modified glass surface, the glass surface was treated with a vinyltriethoxysilane (VTES) coupling agent. First, a 100 mL solution of 5% (v/v) silane in 100% ethanol was prepared. The vinyl silane was purchased from Gelest, Inc. (Tully Town, Pennsylvania, USA) and was used without further purification. To this solution, 5 mL of 0.1 M HCl was added. Separately, the glass substrate was immersed in an acidified ethanol solution (5 mL of 0.1 M HCl added to 100 mL ethanol). The acidified silane solution was then added to the acidified ethanol solution containing the glass substrate to carry out the silane modification reaction. The glass plate was maintained in the reaction solution for 30 min. After the sol-gel treatment, the glass substrate was rinsed with ethanol and dried in air. The plates were subsequently placed in an oven at 110°C for about 30 min to complete the condensation reaction.

A schematic of the experimental apparatus is shown in Figure 1a. An IW-710 INCHWORM motor, from Burleigh Instruments, Inc.

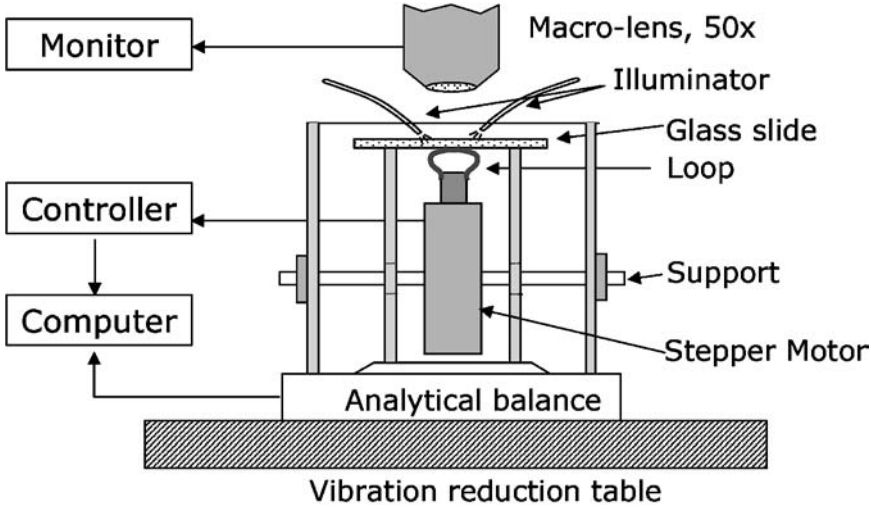


(a)

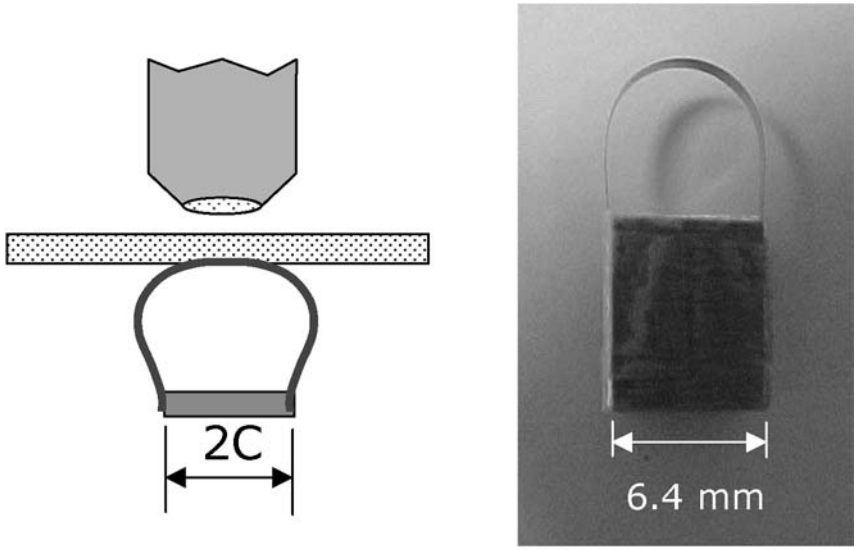


(b)

**FIGURE 1** (a) Schematic of apparatus. (b) Schematic of a loop being brought into contact with substrate. Also shown is a photograph of a typical loop fastened to a test block.

(Fishers, New York, USA), uses compact piezoelectric ceramic actuators to achieve nanometer-scale positioning steps over a range of 6 mm. The motor was supported by an outer polycarbonate cylindrical tube, which rested on the base housing of an SA 210 Scientech (Boulder, Colorado, USA) analytical balance. The substrate, with the surface of interest facing downward, was placed on top of an inner polycarbonate cylinder, which rested on the weight pan of the balance. Just beneath the substrate was the PDMS loop, whose ends were attached to the vertical sides of a block fitted on the shaft of a stepper motor, as shown in Figure 1b. A computer controlled the vertical displacement of the stepper motor, moving the loop into contact with the substrate. The motor displacement was determined through an integral encoder. The optical system used to observe the contact included a macro lens capable of 50× magnification, a gooseneck fiber optic illuminator, and a charge coupled device (CCD) camera connected to a monitor and VCR recorder, as partially shown in Figure 1. A fine scale with 20 μm resolution was set beside the substrate underneath the macro lens for calibration before tests were conducted, and a ruler was then made and attached to the monitor. The entire setup, including the optical system, was placed on a vibration reduction table.



When the loop was pushed against the substrate and then pulled away, the contact zone was observed in the monitor and its dimensions could be determined. At the same time, the contact force between the loop and the substrate could be measured using the analytical balance and recorded automatically by the computer. The motor displacement was determined through an integral encoder and was also recorded by the computer. The computer control program was written in National Instruments LabVIEW 5.0 (Austin, Texas, USA) [10] and used primarily to control the movement of the motor and collect the readings from the balance. The balance was equipped with an RS-232 interface, and a subVI (LabVIEW virtual instrument subroutine) was written to set up a bidirectional communication between the balance and the computer serial port in order to tare the balance and start or stop collecting data. The motor was supplied with a data acquisition board and a control subVI.

Before tests were started, a volume static eliminator VSE 3000 from Chapman Corp. (Portland, Maine, USA) was used to remove static charges through blowing both the loop and the substrate for 10 min. Some time dependence was observed for the contact behavior, so the displacement was prescribed to move in a step fashion. A loading speed of 10.1 μm/s was used for each step, and the sample was allowed to dwell for 200 s between any two steps during the loading cycle. For the unloading cycle, the dwell interval was increased to 300 s per step.

During each step, the displacement was typically changed by 0.05 or 0.1 mm, compressing the loop up to about 1.0 mm.

## EXPERIMENTAL RESULTS

Prior to running tests with the loop, JKR tests were conducted on this apparatus using a PDMS lens coming into contact with a glass substrate coated with PDMS. When the lens moved close to the substrate, it "jumped" into contact, forming a circular contact area. This area increased in size as the motor moved upward, and then decreased as the unloading cycle started. A small hysteresis occurred in the loading and unloading curves of force versus contact radius, similar to that observed for similar material by She *et al.* [11]. The data were analyzed using the JKR theory. A numerical regression method was used to obtain the work of adhesion, $W_a$, which is equal to $2\gamma$ where $\gamma$ is the surface energy of the similar materials in contact, and the parameter $K = 2E/\{3(1-\nu^2)\}$, where E is Young's modulus and $\nu$ is Poisson's ratio. The loading data yielded $W_a = 45.8$ mJ/m$^2$ and $K = 1.73$ MPa, consistent with values given in Chaudhury and Whitesides [12] and Tirrell [13]. For unloading, $W_a$ was found to be 60.2 mJ/m$^2$, which may be high due to energy loss or molecular interdiffusion across the interface, which is not taken into account in the JKR theory.

When the loop is bent, it exhibits anticlastic curvature, meaning that the curvatures parallel and perpendicular to the axis of the loop have opposite signs, resulting in a saddle shape. Figure 2a sketches the case of pure bending of a rectangular beam, for which the radius of

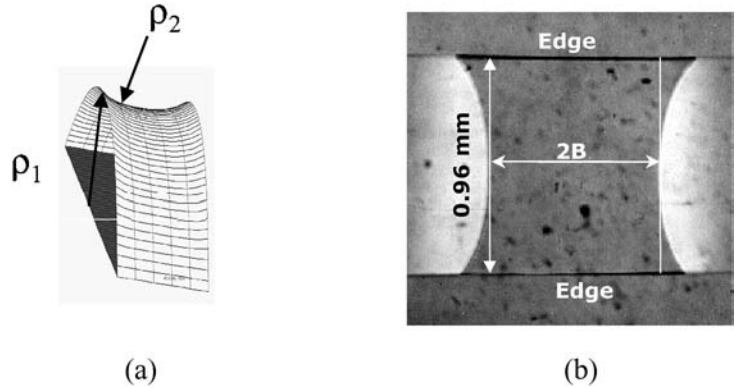


**FIGURE 2** Illustration of (a) anticlastic curvature and (b) observed contact zone of loop with width 0.96 mm and length 2B along centerline.

anticlastic curvature, $\rho_2$, is related to the radius of curvature $\rho_1$ in the plane of bending by Poisson's ratio $\nu$ [14]. Therefore, the substrate is first contacted by the outer edges of the loop halfway between the loop's ends. As the loop mount continues to move toward the substrate, the contact zone spreads across the width of the loop and then propagates outward in the longitudinal direction toward the loop's ends. A typical contact region is depicted in Figure 2b, where "2B" denotes the contact length measured along the centerline of the loop.

The first loop test involved a PDMS loop and PDMS-coated glass substrate. The loop's dimensions were 14.7 mm $\times$ 0.96 mm $\times$ 0.17 mm, and Young's modulus was measured as 1.81 MPa. The horizontal distance between the loop's ends was 6.38 mm. The thickness of the layer of PDMS film on the glass substrate was approximately 0.2 mm. During the unloading cycle, a finite contact area remained when the contact force was zero, and a tensile ("pull-off") force was required to separate the loop from the substrate, analogous to the JKR procedure.



A plot of the contact length *versus* the contact force $F$ is shown in Figure 3a. The length 2B at the centerline is depicted by diamonds (rightmost curve) during loading, and squares (approximately lying on the solid lines) for unloading. The unloading curve almost lies on two straight lines having a constant rate of decrease of the contact length for a while and then a smaller constant rate. The transition in rates occurs when the contact length is about 40% of the width of the loop (denoted by the dashed line). The triangles and filled circles in Figure 3a represent the length of the contact zone at the edges of the strip for loading and unloading, respectively, and are about 0.35 mm larger than the length at the centerline. This ambiguity of the contact length is a distinct disadvantage of the loop method as compared with the JKR method. Unless otherwise noted, the experimental contact width is measured at the loop centerline, as defined in Figure 2.

The relationship of the contact force, $F$, to the vertical displacement, $\delta$, of the ends of the loop is presented in Figure 3b (where $\delta = 0$ for the first measured force after the loop leaped into contact). A small amount of hysteresis is observed. Creep tests and tensile hysteresis tests were conducted on the PDMS material. They indicated that the viscoelastic properties of the material at room temperature contribute little to the hysteresis observed in the loop test. It is believed that the hysteresis is primarily due to the interfacial interactions between the two surfaces. The loop was tested again in a cyclic fashion for three cycles, and the amount of hysteresis increased with the number of cycles [15].

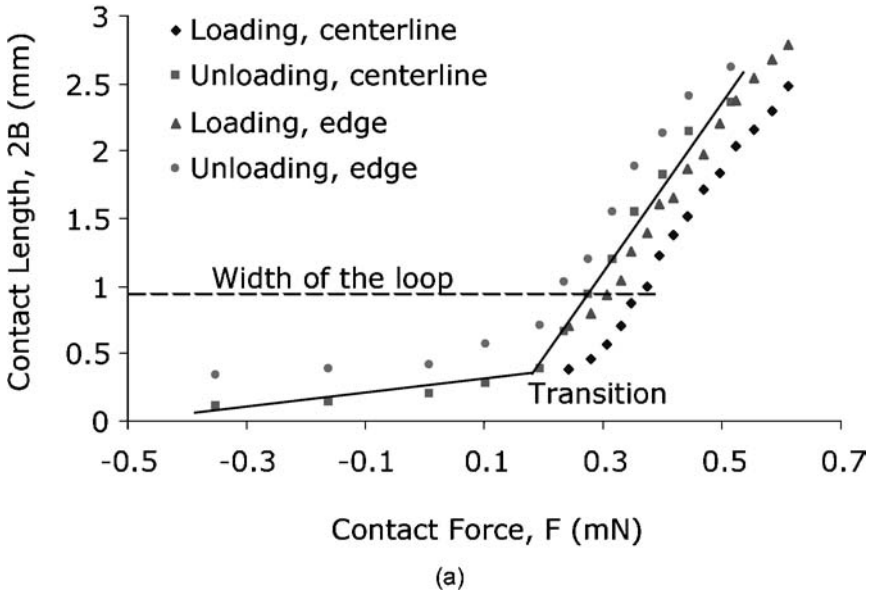


(a)

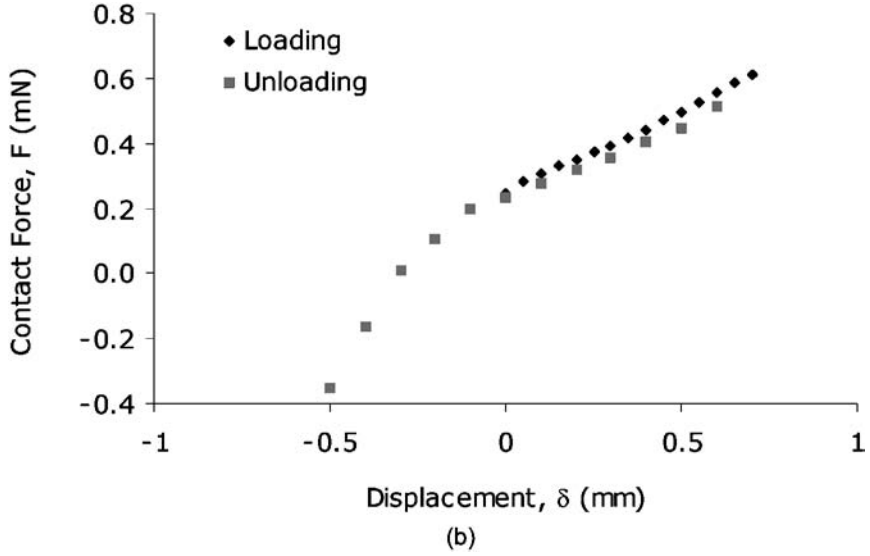


(b)

**FIGURE 3** PDMS substrate: (a) contact length *versus* contact force and (b) contact force *versus* vertical displacement.

The effect of the rate of loading and unloading was also investigated. Rates of 5.1 μm/s and 2 .1 μm/s were applied with no dwell time between steps. The contact length for the higher rate was slightly lower during loading and almost the same during unloading. Therefore, there was more hysteresis at the higher rate, suggesting that the interfacial interaction is a time-dependent phenomenon.

Next, a PDMS loop was pushed onto a glass substrate. The dimensions of the loop were 15.8 mm × 0.94 mm × 0.17 mm. Results are depicted in Figure 4. The straight lines in Figure 4a represent a bilinear fit to the unloading data. The hysteresis or vertical distance between the loading and unloading curves in Figure 4b is much greater than for PDMS on PDMS in Figure 3b (note that the vertical scales in the figures are different by almost a factor of two).

In the third loop test, a smooth polycarbonate plate cleaned with soap, water, and deionized (DI) water was used as the substrate. The loop's dimensions were 15.34 mm × 0.61 mm × 0.21 mm, its modulus was 2.00 MPa, and the distance between its ends was 6.55 mm. The results are shown in Figure 5. After that, a commercial cellulose acetate tape (3 M Scotch™ Transparent Tape 600, 3 M Co., St. Paul, Minnesota, USA) was attached to a glass substrate. The loop had dimensions of 16.8 mm × 0.84 mm × 0.17 mm and a modulus of 1.81 MPa, with its ends a distance of 6.38 mm apart. Figure 6 shows the results for this case.

Finally, four separate treatments of glass substrates were tested, including glass cleaned with acetone, glass sputter-coated with gold or copper, and glass treated with vinylsilane. The results of contact length *versus* contact force are given in Figure 7. The differences in the loading relationships are relatively small. In unloading, the contact lengths are highest for the Cu-treated glass, followed by the acetone-cleaned glass, the vinysilane-treated glass, and the Au-treated glass. The significant differences in the contact lengths during unloading imply that the surfaces are having a substantial effect on the removal process. The very similar behavior for the loading portion of the curves, however, is surprising and not understood at this point.

## FINITE ELEMENT ANALYSIS

A three-dimensional finite element analysis using ABAQUS [16] was conducted to simulate the contact process between the loop and a flat rigid surface. Attractive interfacial forces were not included in the numerical analysis. The loop was assumed to exhibit linearly elastic behavior. Friction between the loop and the substrate was neglected.

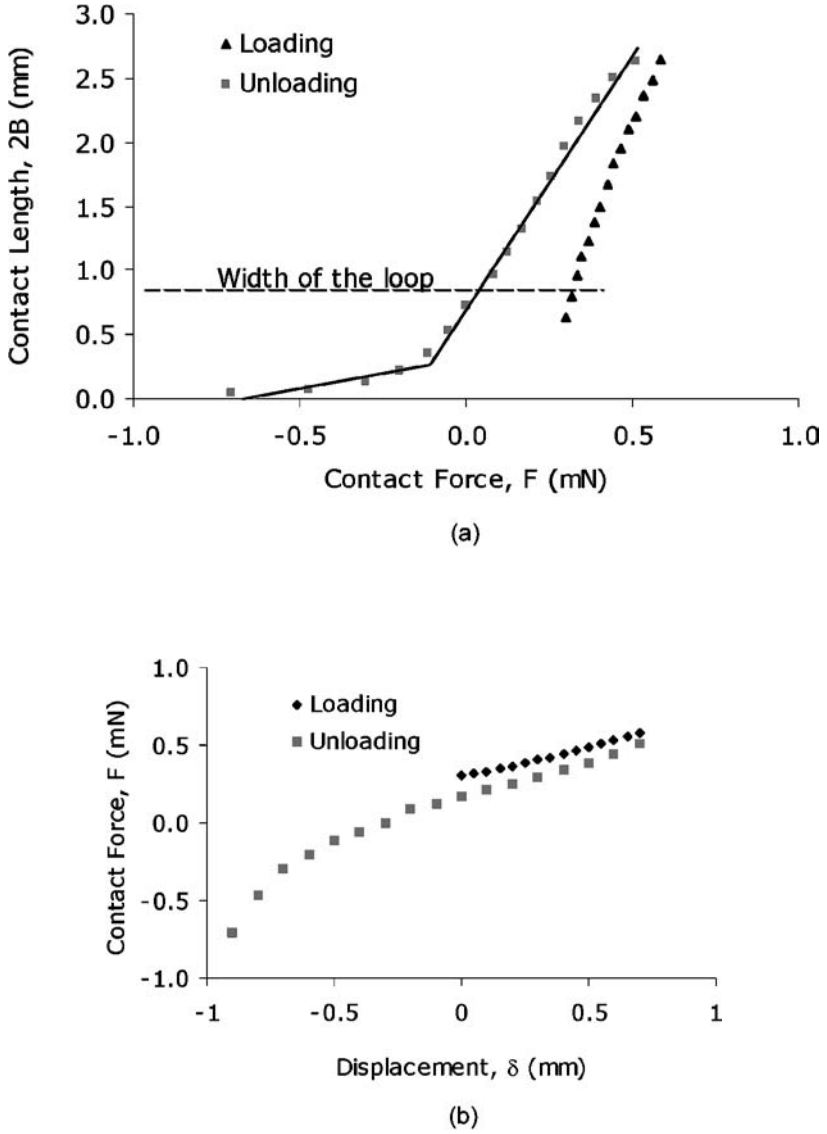




**FIGURE 4** Glass substrate: (a) contact length *versus* contact force and (b) contact force *versus* vertical displacement.

The simulation scheme started with a straight strip. Making use of symmetry, only the right half was modeled. A typical mesh is shown in Figure 8 for a loop with dimensions 14.71 mm × 0.956 mm × 0.165 mm,

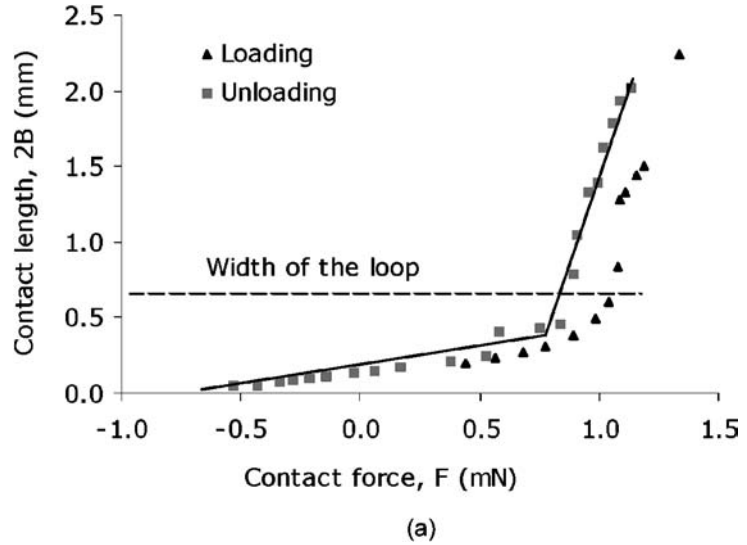


(a)

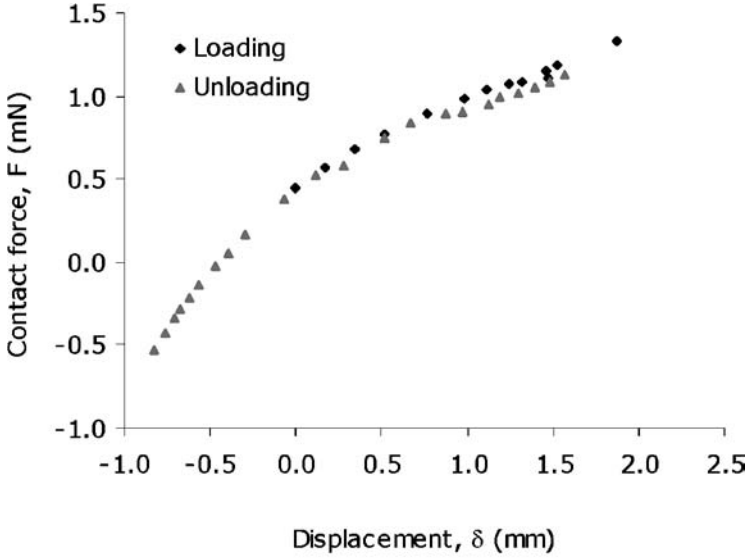


(b)

**FIGURE 5** PC substrate: (a) contact length *versus* contact force and (b) contact force *versus* vertical displacement.

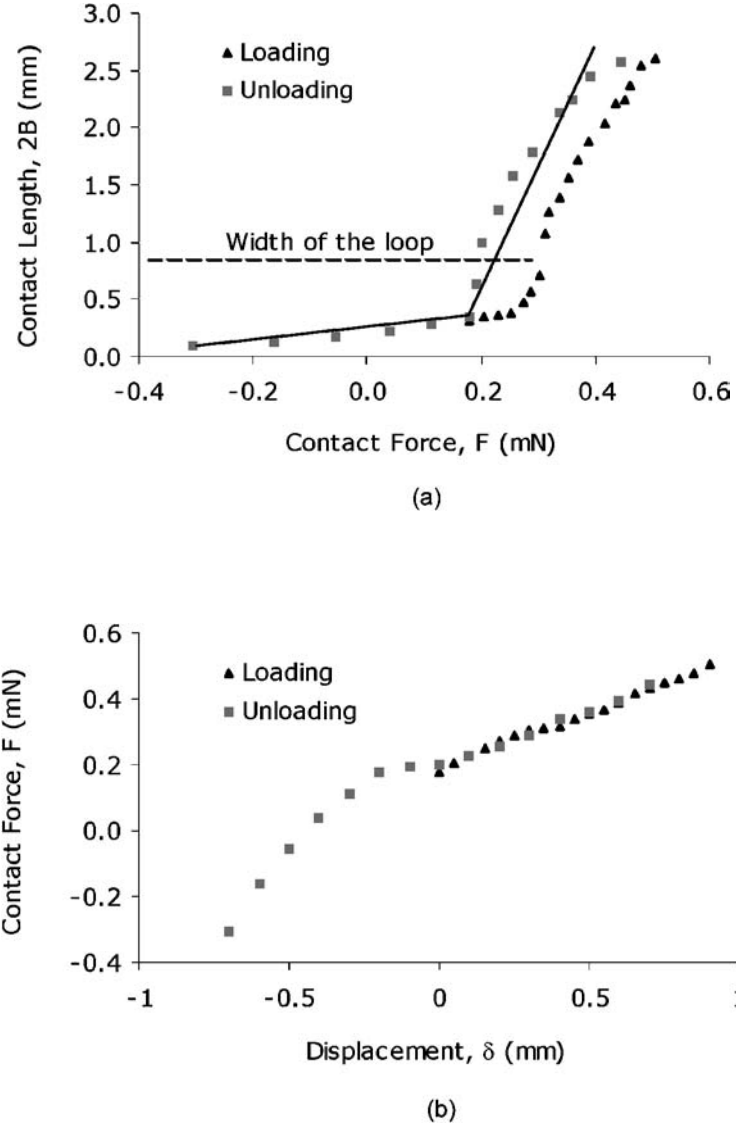


**FIGURE 6** Cellulose acetate substrate: (a) contact length *versus* contact force and (b) contact force *versus* vertical displacement.

Young's modulus of 1.81 MPa, and Poisson's ratio of 0.49. The elements used are S4R four-node shell elements, with a fine mesh in the central region having minimum element size about 0.05 mm × 0.05 mm. The

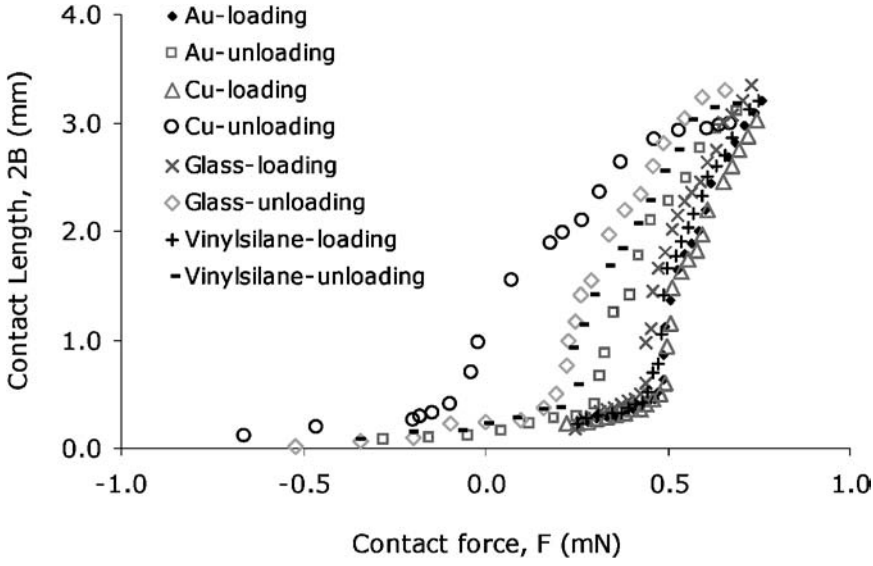


**FIGURE 7** Contact length *versus* contact force for treatments of glass-plate substrate.



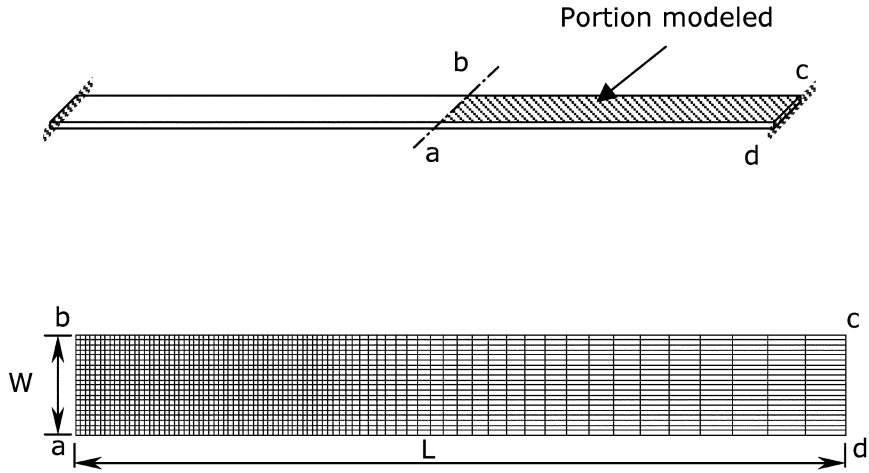


**FIGURE 8** Finite element mesh of loop.

right end of the half-loop was rotated 90° clockwise and moved, until it was 3.19 mm from its left end, horizontally, so the total separation of the loop's ends was 6.38 mm. Anticlastic curvature

occurred, as sketched in Figure 2a. The maximum absolute values of the longitudinal strain (0.034) and transverse strain (0.015) occurred in the center of the loop (*i.e.*, halfway between "a" and "b" in Figure 8).

To model contact in ABAQUS, the loop was defined as the slave surface and the rigid substrate was defined as the master surface. Finite sliding conditions were applied, to be compatible with the geometrically nonlinear model. An iterative contact algorithm was utilized. Small displacement increments of the end of the strip were used, and contact patterns, normal contact stresses, strain distributions, and displacement profiles were obtained.

Figure 9a depicts both the initial form of the contact region after the highest edges of the loop have reached the substrate and a typical spreading contact pattern. The finite element plot shows the right half of the loop, while the inset in Figure 9a presents the experimental result at the corresponding "upper" edge (in the figure) near the center of the loop. As the loop was pushed against the substrate, the form of



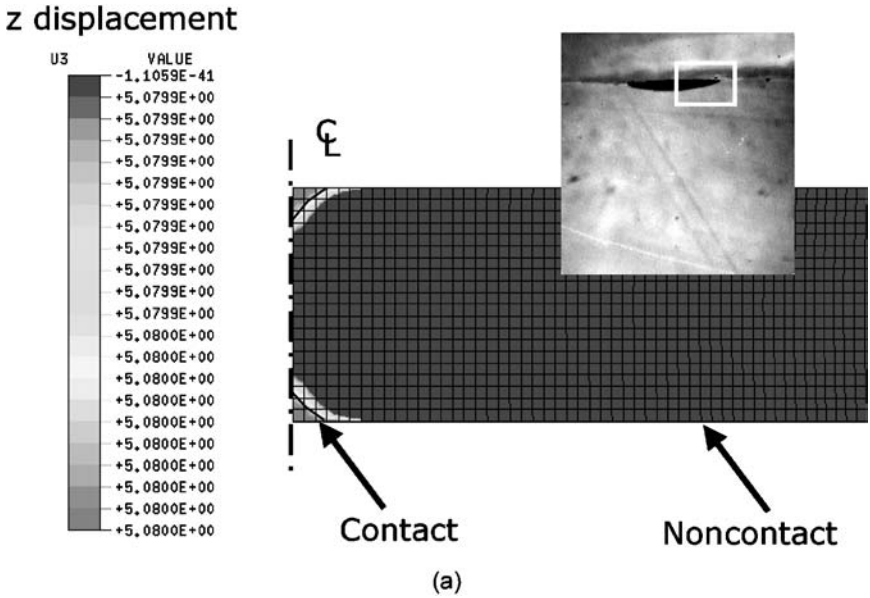


**FIGURE 9** (a) Initial contact region, along outer edges only, from finite element analysis (displacement profiles) and experiment (inset, showing contact region along one edge of specimen. A similar contact zone was observed at the other edge, but out of range in this photo) (see Color Plate I).

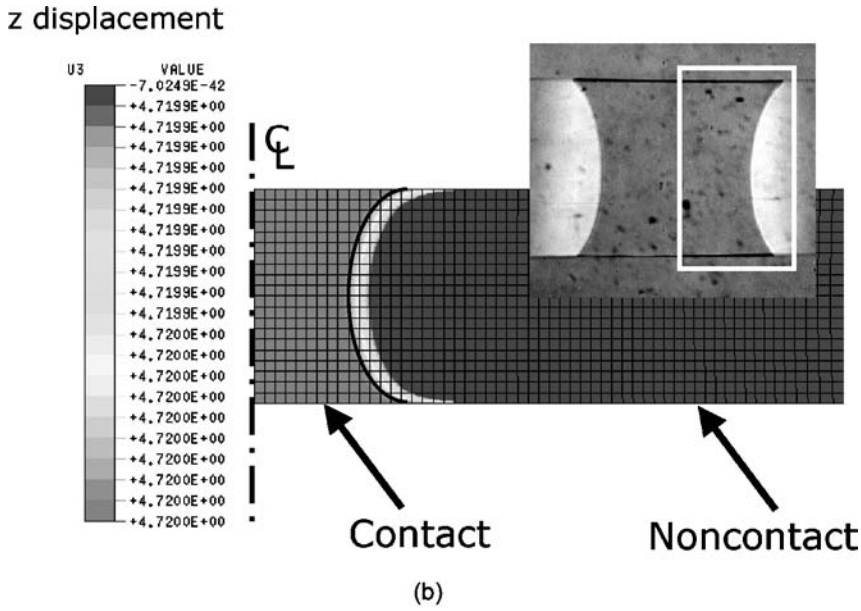


**FIGURE 9** (b) Spreading contact region from finite element analysis (displacement profiles) and experiment (inset) (see Color Plate II).



the boundary of the contact region became similar to the right boundary in Figure 9b. The contact stresses in the contact zone are zero in this analysis, as would be expected since the curvatures of the loop are zero within the contact region.

A typical plot of contact length 2B (along the centerline of the loop) *versus* contact force, *F*, from the finite element analysis is presented in Figure 10. The shape is generally similar to that obtained from the experiments but lacks the bilinear behavior of the experimental plots. Curves using the length at an edge of the strip or at the point of maximum pressure (which is along the edge and slightly within the contact zone) have the same general form [15]. Figure 11 depicts the effect of Poisson's ratio on the contact length. The rightmost data points are the same as in Figure 10, and the other curves demonstrate that the contact length tends to increase as Poisson's ratio decreases (*i.e.*, as the anticlastic curvature decreases). The boundary of the contact zone becomes less curved as $\nu$ decreases and is straight for $\nu = 0$, as would be expected. The corresponding curves for the contact length at an edge or at the point of maximum pressure are less affected by changes in Poisson's ratio [15].

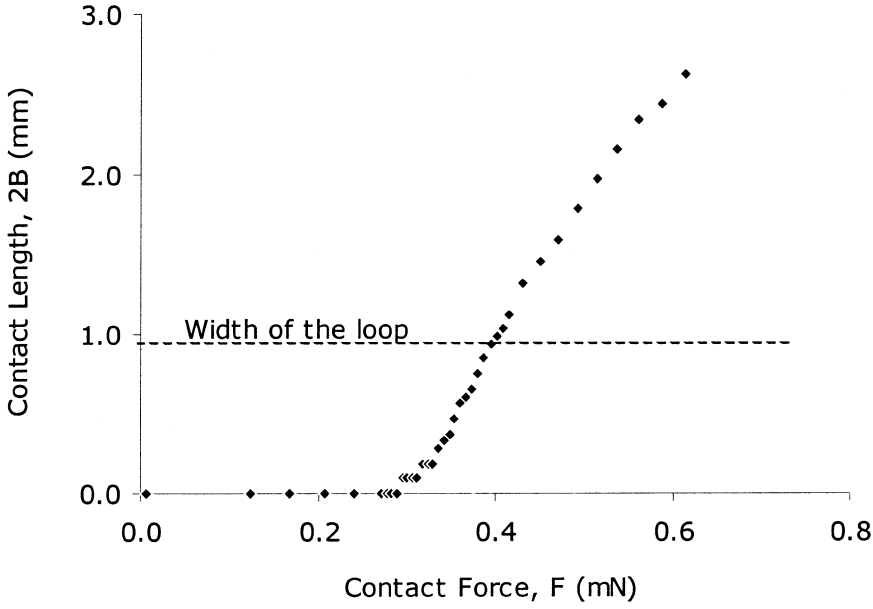


**FIGURE 10** Centerline contact length *versus* contact force from finite element analysis (FEA).

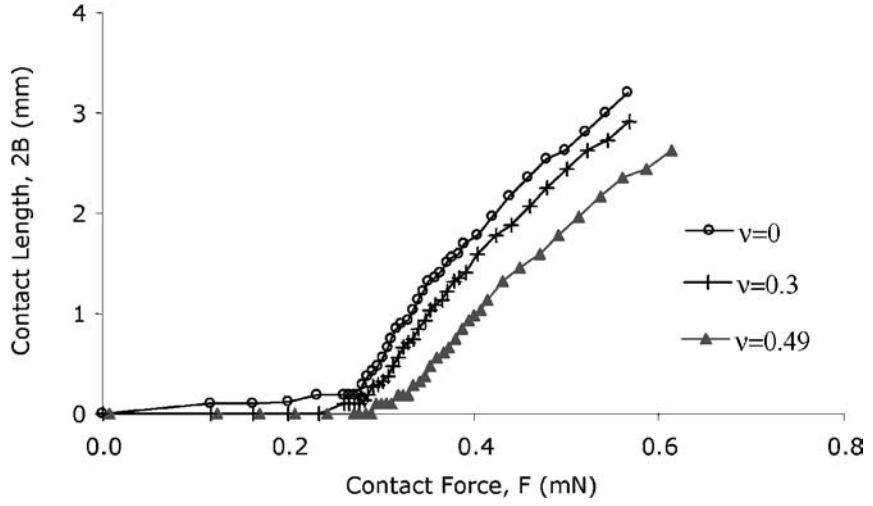


**FIGURE 11** Finite element predictions of the effect of Poisson's ratio on centerline contact length as a function of contact force.

## COMPARISON OF TESTS WITH NUMERICAL ANALYSES

As described in the introduction of this article, a two-dimensional analysis of a linearly-elastic loop contacting a rigid surface was conducted in Plaut *et al.* [7] assuming that the loop was an elastica. Therefore, that analysis did not include extensibility of the loop, anticlastic bending, curvature of the edges of the contact region, or the effect of Poisson's ratio. Contact of the loop with the substrate was assumed to be frictionless. If that analysis is applied to the loop considered in the finite element results of Figure 11, it produces a curve that is almost the same as the one for $\nu = 0.3$ (which uses the contact length at the centerline of the loop).

Figure 12 compares results from experiments, from the finite element analysis, and from the elastica analysis. The experimental results are the same as in Figure 3a for a PDMS loop contacting a plate coated with a PDMS film, using the centerline contact length. FEA denotes the finite element results for the same loop, assuming $\nu = 0.49$, but not including the effect of adhesion between the loop and the plate. The solid curve associated with $\gamma = 0$ is from the elastica analysis when adhesion effects are neglected, and the solid curve corresponding to $\gamma = 21.8\,\mathrm{mJ/m^2}$ is from the elastica analysis using

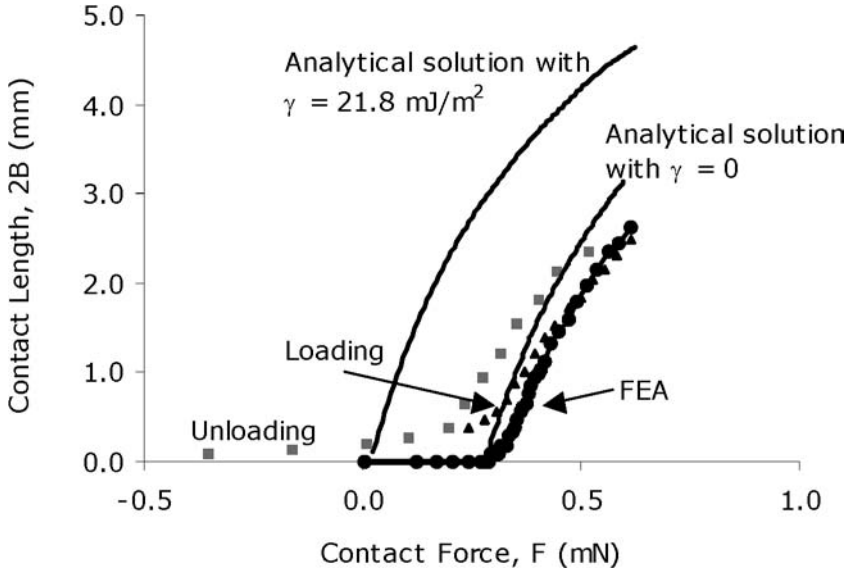


**FIGURE 12** Centerline contact length as a function of contact force from experiments, FEA, and elastica analysis.

a JKR-type of adhesion model and a literature-reported value of surface energy for PDMS [12], with the work of adhesion equal to $2\gamma$ for PDMS on PDMS. This value is similar to what we measured with the JKR method (loading: $\gamma = 22.9\,\mathrm{mJ/m^2}$) and has been used in the earlier analytical work [7].

The experimental results lie close to the finite element results and elastica results when adhesion is neglected. The elastica analysis including adhesion shows much larger contact lengths than observed in the experiments. The analysis of Plaut *et al.* [7] was based on some restrictive assumptions. The curvature of the edge of the contact region is clearly seen in the experimental results (e.g., in Figure 2b) but is not included in the two-dimensional elastica analysis, which cannot include anticlastic bending. A particular type of adhesive model, with no cohesive zone and with concentrated moments at the edges of the contact region, was assumed in the elastica analysis.



## CONCLUDING REMARKS

A flexible loop has been used to try to characterize surface energies of solid surfaces. Results of experiments have been described, in which a PDMS loop was pushed against a substrate and then pulled away from it. The substrates were glass plates coated with PDMS, acetone-washed glass plates, polycarbonate (PC) plates, and a commercial cellulose acetate substrate, plus glass plates treated in different ways. The displacement of the ends of the loop was controlled, and the corresponding contact force was measured. The loop "jumped" onto the substrate, and a "pull-off force" was required to cause separation, as in standard JKR tests. The contact region was observed and seen to possess curved edges due to anticlastic bending of the loop across its width.

In addition, a 3-D finite element analysis was conducted, without including any effect of adhesion. The contact shape predicted numerically was qualitatively similar to that observed experimentally. A two-dimensional analysis using an elastica model of the loop also was utilized for comparison purposes.

Based on a comparison of the experimental results with the two numerical analyses, it appears that the actual contact region for this set of experiments may not be sensitive to the interactive adhesion forces. The contact lengths from the tests are similar to those from the numerical analyses when adhesion effects are ignored. One must wonder whether the loops are achieving and maintaining intimate contact with the substrates for these experiments. Although pressure peaks are expected in the regions where the loop bends to conform to

the flat substrate, no pressure is required within the flat portion of the loop that is actually in contact with the substrate. In other words, along the contact zone, the loop returns to its original straight configuration, so no external forces are required to induce the flat shape. This is in contrast to the spherical or cylindrical JKR probes, where significant pressures are maintained throughout the contact zone. In fact, the maximum contact pressure occurs at the center of the contact zone, maintaining intimate contact and retaining the interfacial energy contributions. The lack of pressure within the flat contact zone of the loop test may fail to keep the loop and substrate in intimate contact. The small work of adhesion energy contribution should be able to hold two ideal surfaces in contact but may not be sufficient to exert this influence for real specimens with imperfections present. This would especially be true for a nonelastomeric loop with small interfacial interactions.

Although analytical models predict the feasibility of the loop method as an alternative technique for measuring work of adhesion values, the experimental results obtained in our laboratory have not been promising. Improved results might be obtained with smaller, more perfect specimens; as one reviewer pointed out, adhesion measurements have been obtained for crossed silica fibers [17]. At this point, however, it is uncertain whether the technique described in this article can be developed into an effective tool for measuring surface energies.



## REFERENCES

[1] Adamson, A. W. and Gast, A. P., *Physical Chemistry of Surfaces* (Wiley-Interscience, New York, 1997).
[2] Johnson, K. L., Kendall, K., and Roberts, A. W., *Proc. R. Soc. London, Ser. A* **324**, 301–313 (1971).
[3] Mangipudi, V. S., Huang, E., Tirrell, M., and Pocius, A. V., *Macromol. Symp.* **102**, 131–143 (1996).
[4] Liechti, K. M., Schnapp, S. T., and Swadener, J. G., *Internat. J. Fracture* **86**, 361–374 (1997).
[5] Shanahan, M. E. R., *J. Adhesion* **63**, 15–29 (1997).
[6] Plaut, R. H., Suherman, S., Dillard, D. A., Williams, B. E., and Watson, L. T., *Int. J. Solids Structures* **36**, 1209–1229 (1999).
[7] Plaut, R. H., Dalrymple, A. J., and Dillard, D. A., *J. Adhesion Sci. Technol.* **15**, 565–581, 2001.
[8] Derjaguin, B. V., Muller, V. M. and Toporov, Y. P., *J. Colloid Interface Sci.* **53**, 314–326 (1975).
[9] Maugis, D., *J. Colloid Interface Sci.* **150**, 243–269 (1992).
[10] LabVIEW 5.0, National Instruments Corporation, Austin, TX (1999).
[11] She, H., Malotky, D., and Chaudhury, M. K., *Langmuir* **14**, 3090–3100 (1998).
[12] Chaudhury, M. K. and Whitesides, G. M., *Langmuir* **7**, 1013–1025 (1991).

[13] Tirrell, M., *Langmuir* **12**, 4548–4551 (1996).
[14] Ashwell, D. B., *J. R. Aeronautical Soc.* **54**, 708–715 (1950).
[15] Qi, J., *MS Thesis*, Virginia Polytechnic Institute and State University, Blacksburg, VA, 2000.
[16] ABAQUS 5.8, Hibbitt, Karlsson & Sorensen, Inc., Pawtucket, RI (1998).
[17] Tomlinson, G. A., *Phil. Mag.* **6**, 695–712 (1928).